Chin. Geogra. Sci.
doi: 10.1007/s11769-014-0722-1

Springer Science Press
www.springerlink.com/content/1002-0063

# Influence of Golmud-Lhasa Section of Qinghai-Tibet Railway on Blown Sand Transport

XIAO Jianhua[1, 2], YAO Zhengyi[1], QU Jianjun[1, 2, 3]

(1. *Key Laboratory of Desert and Desertification*, *Cold and Arid Regions Environmental and Engineering Research Institute*, *Chinese Academy of Sciences*, *Lanzhou* 730000, *China*; 2. *Dunhuang Gobi and Desert Ecology and Environment Research Station*, *Cold and Arid Regions Environmental and Engineering Research Institute*, *Chinese Academy of Sciences*, *Dunhuang* 736200, *China*; 3. *Gansu Center for Sand Hazard Reduction Engineering and Technology*, *Lanzhou* 730000, *China*)

**Abstract:** The Qinghai-Tibet Railway (QTR) passes through 281 km of sandy land, 11.07 km of which causes serious sand damage to the railway and thus, the control of blown sand is important for the safe operation of the railway. Construction of the railway and sand prevention system greatly changed the blown sand transport of the primary surface. Effective and feasible sand-control measures include stone checkerboard barriers (SCBs), sand fences (SFs), and gravel coverings. This study simulated the embankments, SCBs and SFs of the QTR in a wind tunnel, and analyzed their respective wind profile, sand deposition, and sand-blocking rate (SBR) in conjunction with field data, aiming at studying the influence of Golmud-Lhasa section of the QTR and sand prevention system on blown sand transport. The results of wind tunnel experiments showed that wind speed increased by 67.7%–77.3% at the upwind shoulder of the embankment and decreased by 50.0%–83.3% at upwind foot of embankment. Wind speed decreased by 50.0%–100.0% after passing through the first SF, and 72.2%–100.0% after the first row of stones within the first SCB grid. In the experiment of sand deposition, the higher the wind speed, the lower the SBR of SCB and SF. From field investigation, the amount of sand blocked by the four SFs decreased exponentially and its SBR was about 50.0%. By contrast, SCB could only block lower amounts of sand, but had a higher SBR (96.7%) than SF. Although, results show that SFs and SCBs along the Golmud-Lhasa section of the QTR provide an obvious sand blocking effect, they lead to the deposition of a large amount of sand, which forms artificial dunes and becomes a new source of sand damage.

**Keywords:** Qinghai-Tibet Railway (QTR); wind profile; blown sand transport; sand damage; wind tunnel

**Citation:** Xiao Jianhua, Yao Zhengyi, Qu Jianjun, Influence of Golmud-Lhasa section of Qinghai-Tibet Railway on blown sand transport. *Chinese Geographical Science*, doi: 10.1007/s11769-014-0722-1

## 1 Introduction

The Qinghai-Tibet Railway (QTR) is the world′s highest railway, with about 960 km of track located higher than 4000 m above sea level and the highest point 5072 m above sea level. The railway is also the world′s longest plateau railroad, covering 1956 km from Xining City (the capital of Qinghai Province) to Lhasa City (the capital of Tibet Autonomous Region). The newly completed Golmud-Lhasa section zigzags 1142 km across the Kunlun Mountains and Tanggula Range. About 550 km of the track runs on frozen earth (Cheng *et al.*, 2008; Jin *et al.*, 2008). The Golmud-Lhasa section is threatened not only by permafrost, but also by blown sand, both of which can affect the safe operation of the railway (Ma *et al.*, 2009; Xie *et al.*, 2012; Zhang *et al.*, 2012).

Blowing sand can block the operation of trains. Furthermore, sand grains can both permeate mechanical components causing abrasion and decreasing their average number of serviceable years and wear away the

Received date: 2013-12-09; accepted date: 2014-02-28
Foundation item: Under the auspices of National Natural Science Foundation of China (No. 40930741), National Basic Research Program of China (No. 2012CB026105)
Corresponding author: QU Jianjun. E-mail: qujianj@lzb.ac.cn

paint on the exteriors of trains. Thus, sand damage has become an increasingly serious problem for the trains on the QTR (Alghamdi and Al-Kahtani, 2005; Zhang *et al.*, 2010; Bai *et al.*, 2011).

The potential for sand damage along the QTR occurs mainly in highland desert, alpine steppe, and alpine meadow areas. The formation of the surface sand in such areas is different from that in arid desert, semi-arid desert, and Gobi areas (Liu and Zhao, 2001; Zou *et al.*, 2002). The remarkable features of this region are excessively strong winds, low air pressure, alternating freeze-thaw cycles (Wu *et al.*, 2003), poor surface resistance to wind erosion, and sparse short vegetation (Yang *et al.*, 2004). Because of environmental change, especially global warming, glacial retreat, rising snow lines, permafrost degradation, and lake area reduction, some of the wetlands on the Qinghai-Tibet Plateau have become desiccated (Cheng and Wu, 2007; Han *et al.*, 2013). These changes have caused an increase in wind erosion and sand supply, which has resulted in frequent blown sand activity and serious desertification. Sand damage is becoming an increasingly serious problem along the QTR and could become the cause of its first disaster.

Sand fences (SFs) are an effective sand-control measure used extensively in arid land and there are many successful models. Nylon sand fences are used along the Taklimakan Desert Highway and willow branch sand fences are used on the Baotou-Lanzhou Railway. Many researchers have studied the protective mechanisms and benefits of SFs (Qu *et al.*, 2002; Han *et al.*, 2004). Checkerboard barriers are another effective sand-control measure, which can be constructed from a variety of materials, e.g., straw, clay, and salt (Chang *et al.*, 2000). Zhang *et al.* (2012) found that in cold-high environments, sand transport rate increases with increasing wind speed, but decreases exponentially with increasing height in the wind flow. Lots of sand control measures are used to protect the QTR, the longest high-altitude railway in the world (Xu *et al.*, 2006), but there are few researches about their sand-controlling efficiency, and the influence of the QTR and its sand control measures on blown sand transport.

This paper simulated the embankments, stone checkerboard barriers (SCBs) and SFs of the QTR in a wind tunnel, and analyzed their respective wind profile, sand deposition, and sand-controlling efficiency in conjunction with field data. The results of this paper will be useful for identifying the influence of the Golmud-Lhasa section of the QTR on blown sand transport, and for guiding improvements in future designs of sand-control measures.

## 2 Study Area

Most of the study area is located higher than 4000 m above sea level in an alpine arid and semi-arid area. Annual precipitation is 250–300 mm (Wu and Zhang, 2010). The climate is dry, and strong winds are a significant feature. Winter on the plateau persists for 6–9 months, and during this time, the winds are predominantly from the west. Some of the strongest winds in China were recorded in some areas along the Golmud-Lhasa section of the QTR. In Tuotuohe**,** strong winds occur 167.8 days annually with a maximum sustained wind speed of 30 m/s and a maximum instantaneous wind speed of 40 m/s (Bai *et al.*, 2005). The strong winds are concentrated mainly from December to next May, accounting for 58% of the annual total. However, only 27.2 mm of precipitation occurs during this time, which is less than 10% of the annual total (Zhang *et al.*, 2011). In Amdo, the annual maximum sustained wind speed is 38 m/s with 148.8 strong wind days (Bai *et al.*, 2005). Wudaoliang experiences an average of 135.5 days of strong wind with a maximum sustained wind speed of 31 m/s and maximum instantaneous wind speed of 40 m/s (Bai *et al.*, 2005), concentrated in winter and spring. In Cuona Lake, the sand-driving wind occurs mostly from December to next April, which accounts for 65% of the annual total (Ying *et al.*, 2013). In addition to the dry air during this time, the dry ground accelerates the desertification process. Sand drift is the dynamic condition of wind erosion and the train has overturned phenomenon in sand storm areas. Most area along the QTR is alpine steppe and alpine meadow whose vegetation is sparse and the ecological environment is fragile. The construction of Qinghai-Tibet highway and railway severely destroyed natural vegetation and landscape, especially in 50 m wide buffer regions along the roads (Chen *et al.*, 2003). Based on early field investigations in October 2006 and August 2007, and combined with an analysis of aerial photography, we found that the total lengths of sand damage along the Golmud-Lhasa section of the QTR is 269 677 m. Severe, moderate, and mild levels of sand

damage occur over lengths of 10 335, 49 834, and 209 508 m, respectively, which account for about 3.8%, 18.5%, and 77.7% of the total, respectively. Severe and moderate sections of sand damage are located mainly at Honglianghe, Xiushuihe, Tuotuohe, Tongtianhe, and the Cuona Lake, and light sand damage is concentrated in the section between Wudaoliang and Golmud (Fig. 1).

Figure 2 shows the sand-control measures employed at the Cuona Lake. These include SFs, SCBs, and gravel coverings. Field survey results show that the SFs and SCBs along the Golmud-Lhasa section of the QTR have accumulated large amounts of sand and provide an obvious sand-blocking effect. The sand-prevention system at the Cuona Lake shows the highest accumulation.

## 3 Experimental Setup and Model

Based on the sand-prevention system along the Golmud-Lhasa section of the QTR, we simulated the railway embankment, SCBs, and SFs in a wind tunnel. We tested their wind flow and amount of sand accumulation for the latter two models in the wind tunnel as well as in the field.

### 3.1 Wind tunnel simulation

The experiments were conducted in a blowing sand wind tunnel at the Key Laboratory of Desert and Desertification, Chinese Academy of Sciences. The wind tunnel was used primarily to simulate blowing sand and surface flow. The total length of the blow-type non-circulating wind tunnel is 40 m with a 21-m-long test section. The cross-sectional area of the test section is 1.2 m × 1.2 m. The free-stream wind speed in the wind tunnel ranges from 1 m/s to 40 m/s. Wind speed is measured with a Pitot tube connected to a pressure sensor and data acquisition system, and the data were recorded automatically on a portable computer (Fig. 3a). The model was installed in the wind tunnel test section, as shown in Fig. 3b. The Pitot tube has 10 inductors at heights of 0.3 cm, 0.6 cm, 1.2 cm, 1.6 cm, 3.0 cm, 6.0 cm, 12.0 cm, 20.0 cm, 35.0 cm, and 50.0 cm, respectively (Fig. 3c).

To facilitate the blown sand experiment, a 4-m-long × 3-cm-thick × 100-cm-wide sand bed was placed upwind of the SCB and SF models. The sand deposited in and around each SCB and that at the front and rear of the control fences were weighed. The sand bed was replenished after each trial at a given wind speed.

### 3.2 Railway embankment model

A typical cross section of the embankment with side slopes of 1.5 : 1 (horizontal : vertical) is shown in

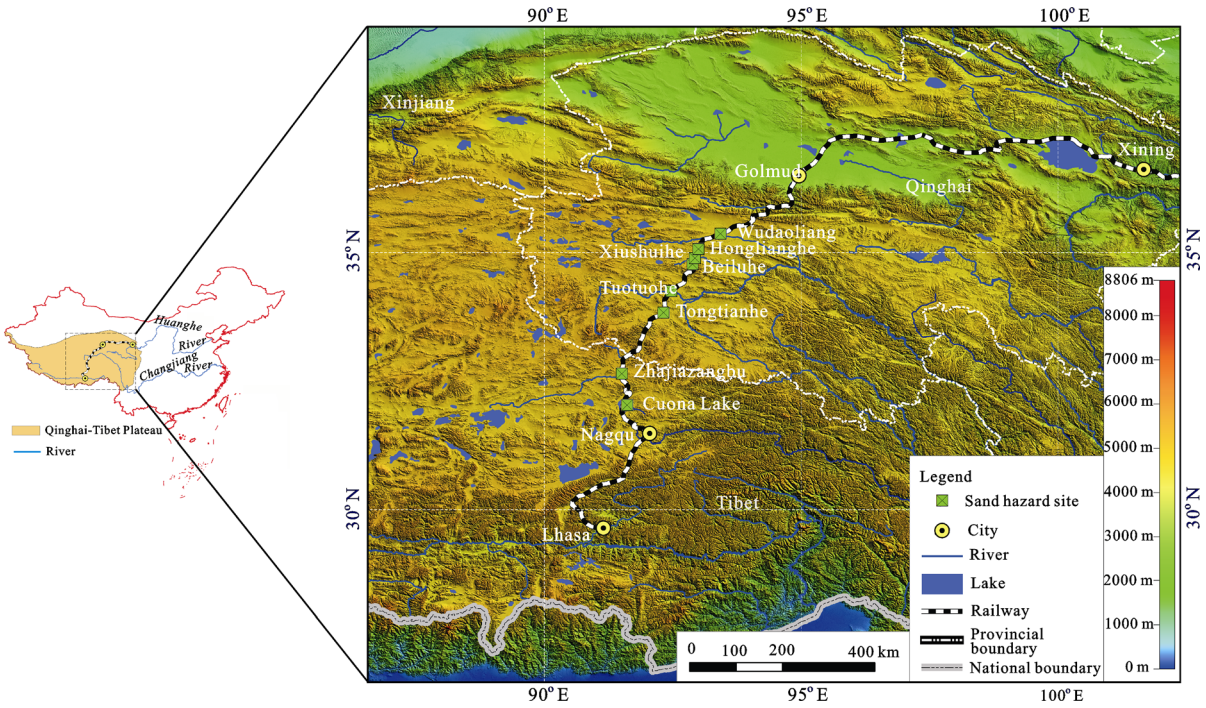


**Fig. 1** Golmud-Lhasa section of Qinghai-Tibet Railway (QTR)

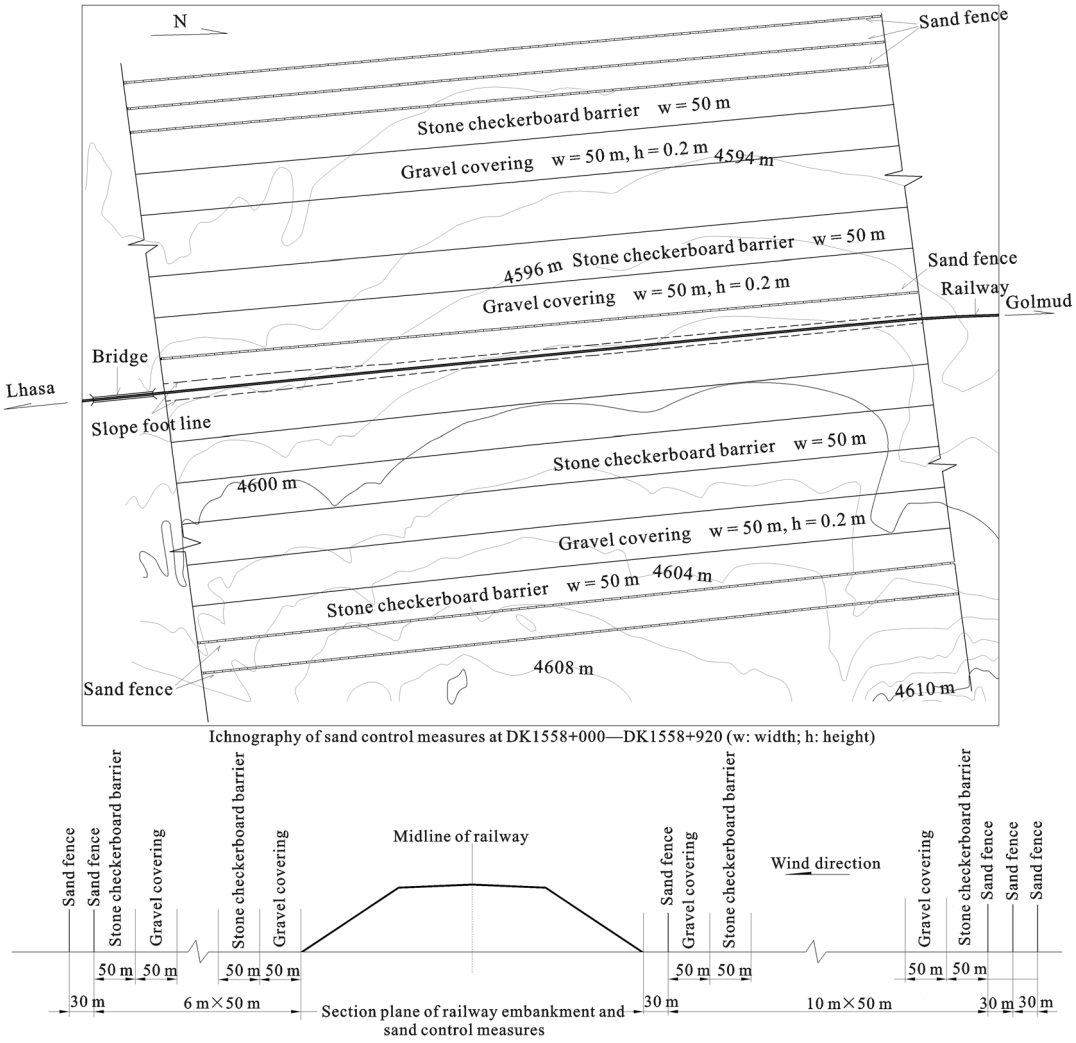


**Fig. 2** Typical sand-control measures at Cuona Lake, from DK1558+000 to DK1558+920 along QTR. DK refers to mileage identifier of QTR

Fig. 3b. This cross section is from Tuotuohe in the Golmud-Lhasa section of the railway. The height of this section is 8.14 m, and its top and bottom widths are 3.7 m and 31.8 m, respectively. A two-dimensional 1 : 20-scale trapezoidal model of the embankment was adopted. The model was constructed of wood panels with surface roughness values low enough to be considered a smooth surface. The model was 25.1-cm high, and its top surfaces were 37-cm long; slope gradients were 1.5 : 1 (horizontal : vertical) with slope angles of 33.7°. The downstream and upward directions were defined as positive, and the origin was set at ground level at the center of the embankment top. Figure 4a shows the railway embankment model in the wind tunnel.

### 3.3 Stone checkerboard barrier (SCB) model

The model was 1 : 1-scale with a stone grid size of 1.00 m × 1.00 m × 0.15 m (length × width × height) (Fig. 4b). The model contained three SCBs. Measurements of the model were taken continuously along the wind tunnel axis. The 16 measuring points were located at 3H and 1H before and at 0H and 1H after the first row of stones; at 1H before and at 0H and 1H after the second row of stones; at 1H before and at 0H, 1H, and 3H after the third row of stones; at the midpoints of the first and second SCBs; and on the top of the first, second, and third row of stones along the wind tunnel axis (H = 15 cm, which is the height of the SCBs). In the wind tunnel experiments, each measuring point along the cross section of the centerline was at a different height. In the wind speed change experiment, three wind speeds (10 m/s, 15 m/s, and 20 m/s) were selected, and it took 10 minutes respectively. In the sand deposition distribution experiment, four wind speeds (8 m/s, 10 m/s, 12 m/s

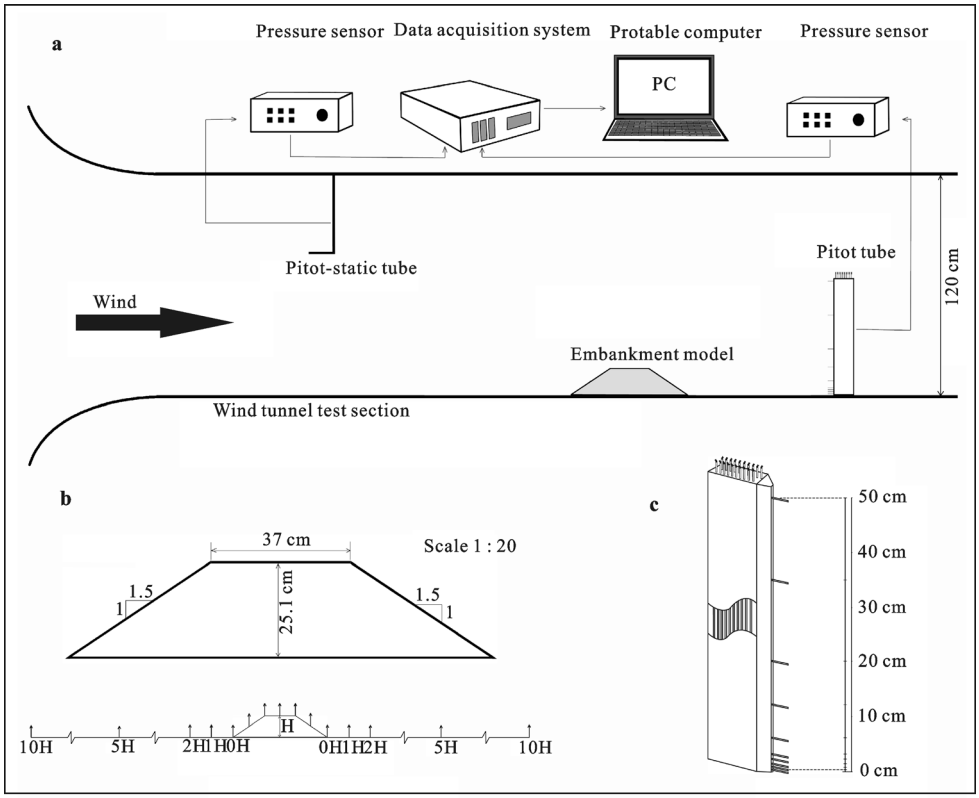


**Fig. 3** Schematic of wind speed measurement system and experimental setup. a, wind speed measurement system; b, embankment model; and c, Pitot tube. H means the height of embankment


**Fig. 4** Experimental models in wind tunnel. a, railway embankment model; b, SCB model; and c, SF model

and 15 m/s) were selected, and it took 10 minutes respectively, and the wind speed of 10 m/s took another 20 minutes contrast experiment.

### 3.4 Sand fence (SF) model

Two SFs models were installed and their structure and experimental layout are shown in Fig. 4c. The height, width, and thickness of the model were 45 m, 120 cm, and 1.2 cm, respectively. Therefore, the model can be considered a two-dimensional obstacle, and two-dimensional measurements (horizontal and vertical) are sufficient to reveal the characteristics of the speed and turbulence produced when the models are positioned perpendicular to the wind. The fences can also be considered thin obstacles, such that the effect of the downwind edges of the fences on flow separation is negligible.

The experiment incorporated 11 measuring points on the top of and at 0.5H, 1H, 2H, 4H, and 6H both before and after the fence along the wind tunnel axis. In the wind speed change experiment, three wind speeds (10 m/s, 15 m/s, and 20 m/s) were selected, and it took 10 minutes respectively. In the sand deposition distribution experiment, five wind speeds (8 m/s, 10 m/s, 12 m/s, 14 m/s, and 16 m/s) were selected, and the experiment time of each wind speed is 10 minutes.

periment time of each wind speed is 10 minutes.

## 4 Results

### 4.1 Wind speed change in wind tunnel experiment

#### *4.1.1 Railway embankment*

Figure 5 shows the wind profile across the railway embankment. The highest wind speed area is formed at the upwind shoulder of embankment. Wind speed increases by 67.7%–77.3% at the upwind shoulder of embankment and decreases by 50.0%–83.3% at upwind foot of embankment that is the lowest wind speed at the upwind of embankment. The wind speed decreases by 66.7%–100.0% at the downwind side of embankment, where forms a large area of low wind speed area. As the airflow approaches the railway embankment, the wind speed decelerates at the foot of the embankment on the upwind side, and increases as the airflow goes up the slope of the embankment, reaching a maximum at the embankment shoulder. Furthermore, it forms a decelerated depositing region immediately downwind of the embankment. In the field, the blown sand will firstly deposit at upwind foot of embankment. Then it will go up to the upwind of the embankment where part of it will be flowed into the air by its high wind speed, and part of the sand will deposited in the railway rail because the rail have a blocking effect. At last, the sand flowing into the air and passing through the rail will deposit at the downwind side of embankment.

#### *4.1.2 Stone checkerboard barriers (SCB)*

The wind tunnel experiment contour map is shown in Fig. 6 with experimental wind speeds of 10 m/s, 15 m/s, and 20 m/s. The wind speed near the SCB has a similar triangular distribution pattern, which is affected by the first row of stones, forming a wind speed-reduction zone. At the top of the first row of stones, wind speed increases by 28.6%–33.3% significantly. After the first row of stones in the first SCB grid, there is a region of significantly lower speed below the height of 25 cm and wind speed reduces by 72.2%–100.0%.

#### *4.1.3 Sand fence (SF)*

The wind tunnel experiment shows that wind profile exhibit substantially the same distribution pattern under the different experimental speeds (Fig. 7). Affected by the fence, a triangular speed-reduction zone is formed

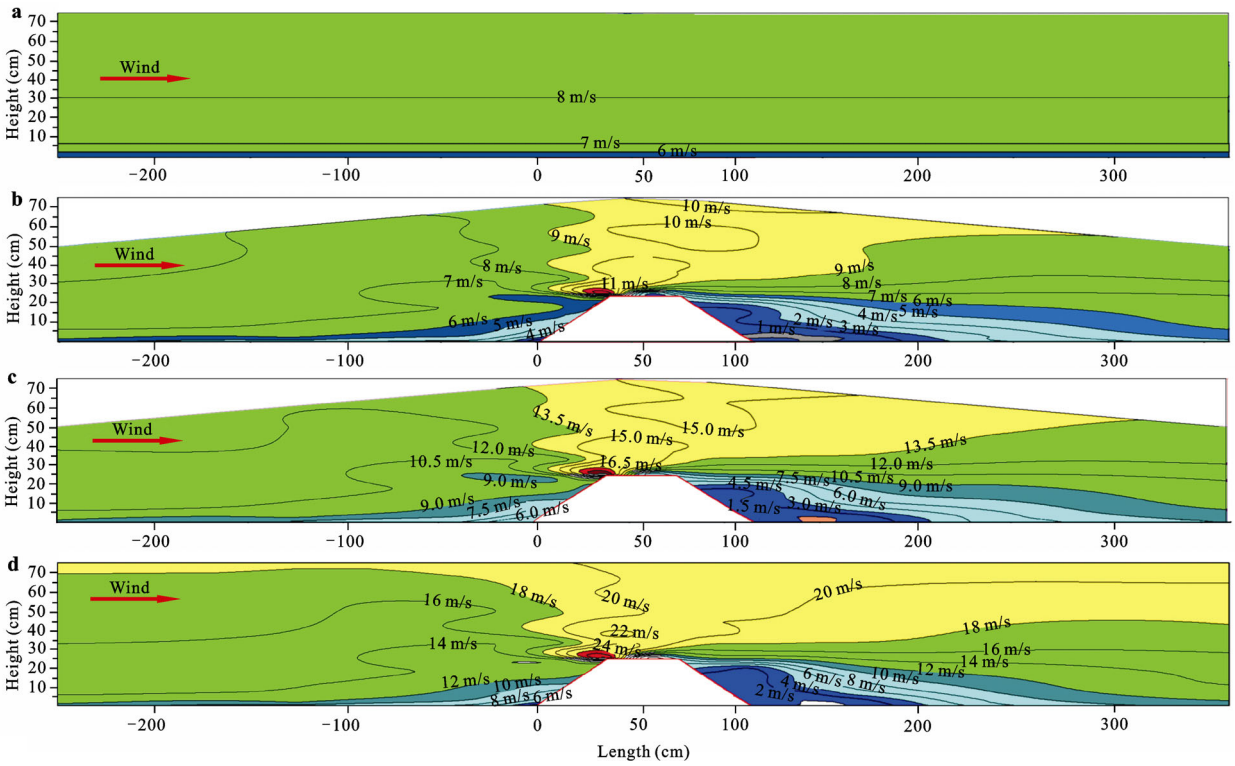


**Fig. 5** Wind profile across railway embankment. a, before placement of experimental model, wind speed of 10 m/s; b, after placement of experimental model, wind speed of 10 m/s; c, after placement of experimental model, wind speed of 15 m/s; and d, after placement of experimental model, wind speed of 20 m/s

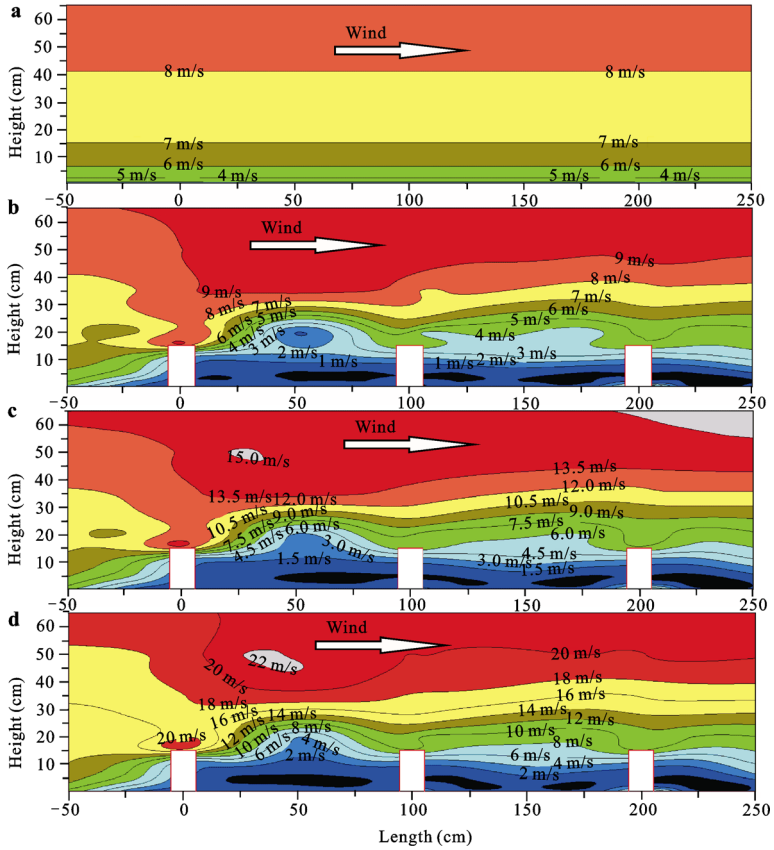


**Fig. 6** Wind profile across stone checkerboard barriers (SCBs). a, before placement of SCBs model, wind speed of 10 m/s; b, after placement of SCBs model, wind speed of 10 m/s; c, after placement of experimental model, wind speed of 15 m/s; and d, after placement of experimental model, wind speed of 20 m/s

upwind of the fence. Above the fence, wind speed increases by 25.0%–50.0%. Downwind of fence, about 0.7–1.2 H high, wind speed decreases significantly, by 50.0%–100.0%. At the bottom of the fence, wind speed increases slightly, mainly because of the larger opening underneath.

## 4.2 Sand deposition distribution in wind tunnel experiment

### *4.2.1 Stone checkerboard barriers (SCB)*

The distribution of sand deposition in the SCB shows an obvious regularity (Fig. 8). The sand-blocking rate (SBR) is the ratio of sand deposition in the SCB to the total amount of sand. The results of wind tunnel experiments showed that at different wind speeds, the amount of sand deposition in the different stone squares was different, and that the higher the wind speed, the lower the rate of sand blocking (Table 1). Furthermore, extending the test time reduced the SBR. As shown in Fig. 9, the distribution of sand deposited in the SCBs presents an obvious regularity with a power function distribution, exhibiting high correlation coefficients except when the wind speed is 10 m/s (Table 2).

**Table 1** Sand-blocking rate for stone checkerboard barrier (SCB) model

| Wind speed (m/s) | Duration time (min) | Sand-blocking rate (%) | | | |
|---|---|---|---|---|---|
| | | First grid | Second grid | Third grid | Total |
| 8 | 10 | 61.21 | 18.20 | 8.94 | 88.35 |
| 10 | 10 | 58.17 | 17.29 | 8.50 | 83.96 |
| 12 | 10 | 47.22 | 13.19 | 6.93 | 67.34 |
| 15 | 10 | 27.45 | 7.72 | 4.04 | 39.22 |
| 10 | 20 | 45.48 | 14.74 | 7.28 | 67.49 |

**Table 2** Sand deposition distribution parameter for stone checkerboard barriers (SCBs)

| Wind speed (m/s) | Function relationship | Correlation coefficient ($R^2$) |
|---|---|---|
| 8 | $y = 2.56x^{-2.06}$ | 0.9901 |
| 10 | $y = 3.96x^{-0.63}$ | 0.8916 |
| 12 | $y = 9.41x^{-1.5}$ | 0.9998 |
| 15 | $y = 16.87x^{-1.8}$ | 0.9943 |

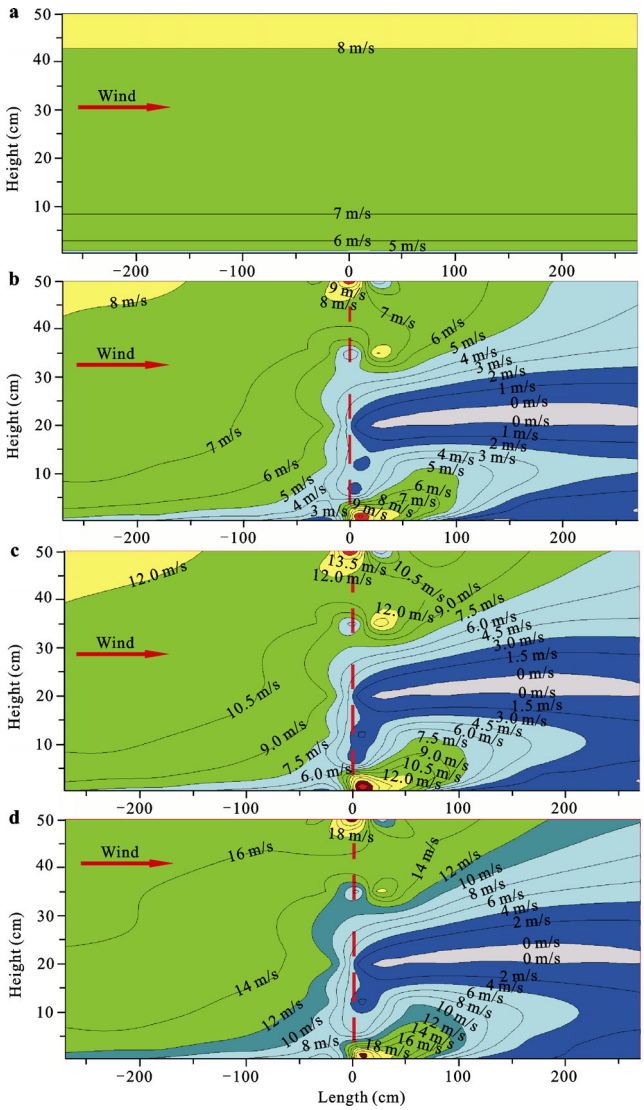


**Fig. 7** Wind profile across sand fence (SF). a, before placement of experimental model, wind speed of 10 m/s; b, after placement of experimental model, wind speed of 10 m/s; c, after placement of experimental model, wind speed of 15 m/s; and d, after placement of experimental model, wind speed of 20 m/s

### *4.2.2 Sand fence (SF)*

Because of the limiting length of the wind tunnel, only two SFs were set up (Fig. 4c, Fig. 10). Therefore, we were unable to report on the relationship of the amount of sand deposited between each fence. The SBR describes the ratio of the amount of sand deposited upwind and downwind of the fence to the total amount of sand. In the wind tunnel tests, the ratio of the amount of sand deposited between two fences to the total amount of sand can be approximated as a replacement of the SBR. The results of wind tunnel experiments showed that the SBR of the SF was different at different wind speeds; the higher the wind speed, the lower the SBR (Table 3).


**Fig. 8** Sand deposition in stone checkerboard barriers (SCBs) in wind tunnel experiments. a, before first SCB; b, inside first SCB; c, inside second SCB; and d, inside third SCB

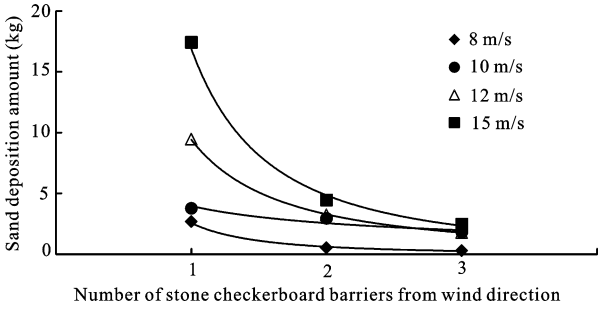


**Fig. 9** Distribution of sand deposited in stone checkerboard barriers (SCBs)

**Fig. 10** Sand deposition in sand fence (SF) in wind tunnel experiments

**Table 3** Sand-blocking rate for sand fence (SF) model

| Wind speed (m/s) | Duration time (min) | Sand-blocking rate (%) |
|---|---|---|
| 8 | 10 | 95.62 |
| 10 | 10 | 94.21 |
| 12 | 10 | 92.91 |
| 14 | 10 | 90.21 |
| 16 | 10 | 84.83 |

### 4.3 Sand-controlling efficiency measured in field

The results of field survey showed that SFs and SCBs along the Golmud-Lhasa section of the QTR have accumulated large amounts of sand and that they provide an obvious sand-blocking effect (Fig. 11). Sand-controlling efficiency is determined by measuring the amount of sand deposition that is blocked by a sand-control measure. In the field investigation, it was found that where sand deposition had the maximum length, it had maximum thickness. Figure 12 shows schematics of sand deposition downwind of the SF. The profile of the deposited sand was similar to a triangle and thus, by measuring the lengths and height of the triangle, the area could be calculated. We can use the area of the profile triangle, multiplied by 1 m, to represent the amount of sand deposited per unit width. We measured the maximum length ($L$) and the maximum thickness ($H$) of the sand deposit and calculated the deposited amount ($S$) using the following equation:

$$S = 0.5 \times L \times H \quad (1)$$

Field investigation results showed that the SFs were highly efficient at blocking sand. As shown in Table 4, in Honglianghe, the total amount of sand deposition along the four fences was 26.5 $m^3$/m. Although the first fence had lost its efficacy, sand deposited along the other three fences had not reached half the height of that deposited along the first fence. At the Cuona Lake, the amount of sand deposited along the four fences was 150.9 $m^3$/m. The thickness of the sand at the three fences closest to the lake was 2 m and the fences were buried. The total amount of sand deposited along these three fences was 149 $m^3$/m, showing that fences are highly effective at blocking sand.

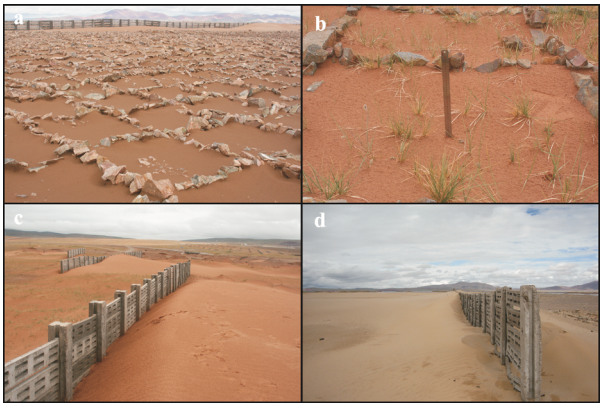


**Fig. 11** Photographs of stone checkerboard barriers (SCBs) and sand fences (SFs). a and d in Cuona Lake; b and c in Honglianghe

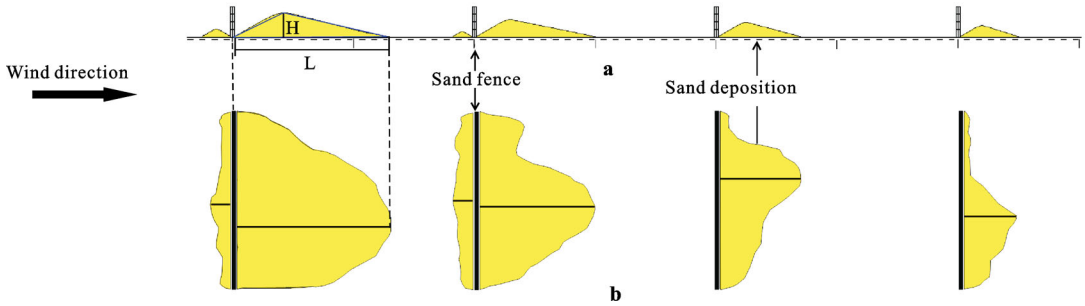


**Fig. 12** Schematic of sand deposition by sand fences (SFs). a, side view; b, top view. H is the maximum thickness and L is the maximum length of sand deposit

**Table 4** Amount of sand accumulated by each sand prevention system

| Position | SCB | | | SF | |
|---|---|---|---|---|---|
| | Total width (m) | Average thickness (cm) | Maximum amount of sand accumulation ($m^3$/m) | Total number | Maximum amount of sand accumulation ($m^3$/m) |
| Honglianghe | 75 | 14.97 | 14.1 | 4 | 26.5 |
| Xiushuihe | – | 5.67 | – | – | – |
| Left bank of Beilu River | – | 13.76 | – | 4 | 17.3 |
| Right bank of Beilu River | – | 8.70 | – | 3 | 15.3 |
| Left bank of Tuotuo River | 200 | 6.78 | 13.6 | 4 | 14.8 |
| Left bank of Tongtian River | 90 | 5.00 | 4.5 | 2 | 15.2 |
| Zhajiazangbu | – | – | – | 2 | 8.3 |
| Cuona Lake | 250 | 14.20 | 35.5 | 4 | 150.9 |

Note: '–', the data are omitted where there is no SCB or SF

Compared with the SFs, the SCBs are less effective at blocking sand. In Honglianghe, the SCBs are 75 m wide, and the sand thickness ranges from 10 cm to 25 cm with an average thickness of 14.97 cm. The amount of sand deposited within the SCBs is calculated to be 14.1 $m^3$/m. When the thickness of the sand within the SCBs is higher than 15 cm, its sand-controlling efficiency will greatly reduce. The maximum thickness of the sand in the SCBs is 25 cm, with an average thickness of nearly 15 cm. Thus, the SCBs reach their limit and their sand-controlling efficiency greatly reduces. In this area, the SCBs are ineffective.

The amount of sand deposited at the four SFs is 1.88 times that deposited within the SCBs, under the condition that the amount of sand deposited at three of the SFs has not reached maximum capacity. If all four fences reach maximum capacity, the amount of sand deposited at the four fences would be 3.68 times that deposited within the SCBs. At the Cuona Lake, west of the railway, the amount of sand deposited at the four fences is 4.25 times that deposited within the five SCBs. By comparing the amounts of deposited blocked sand, the sand-controlling efficiency of the SF is better than that of the SCBs.

However, the SFs have gaps and some sand can pass through the fence gaps or over the fence. Therefore, fences can not fully reduce the strength of the sand flow, although some sand is blocked. In field, the SBR can be calculated by the blown-sand activity intensity decreased by the sand-control measure. Wind activity monitoring in Tuotuohe showed that blown-sand activity intensity is generally higher than 2282.8 g/$cm^2$ in original sand land. However, blown-sand activity intensity downwind of a SF is 1059.8 g/$cm^2$, which is about half that of original sand land. Therefore, the SBR of a SF is about 50%. In Honglianghe, the amount of sand blocked by the four SFs decreases exponentially (Fig. 13) and thus, the SBR of a SF can be calculated as approximately 50%. When the SF is unable to block more sand, the rate of sand deposition is greatly reduced. The results of field survey showed that when sand thickness at the first fence is 1 m or more, the SBR is greatly attenuated, allowing sand to cross the first fence and accumulate at the second and third fences. Thus, use of SFs alone can not block all of the sand.

A SCB can only block small amounts of sand, but it has a higher SBR. By monitoring blown sand, it can be found that when combined with the SFs, the SCBs can reduce the blown-sand activity intensity to 1/30 of that of original sand land. It indicates that the SCB has a higher SBR which is about 96.7%. When the thickness of accumulated sand within the SCB is close to the height of the stones, the SCBs are effectively buried and they lose their sand-blocking function. Sand continues to accumulate within the SCBs, and if not removed, this accumulated sand will be transformed into a new sand source that will continue to threaten the railway. The activity of wind-blown sand in Tuotuohe and other areas fully illustrates this point. Further control of sand damage will require new controlling measures.

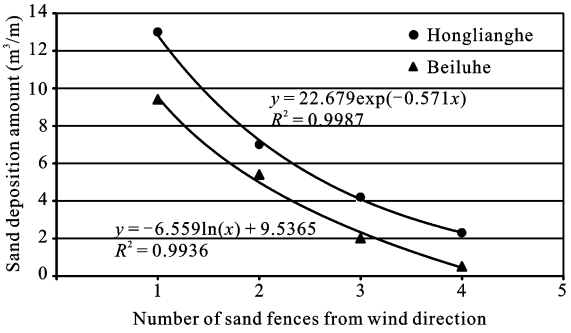


**Fig. 13** Sand deposition amount decreases in four sand fence (SFs) in Honglianghe and Beiluhe

## 5 Discussion and Conclusions

Many transport lines, such as the Shapotou section of the Baotou-Lanzhou Railway and the oil transport highway in the Taklimakan Desert, are subjected to severe damage from sand. The Shapotou section is an area that combines typical vegetation and engineering measures based on the principle of ′relying mainly on fixation, and combined blockage′. This is a pioneering work in sand-hazard control in China (Qiu *et al.*, 2004; Zhang *et al.*, 2007). In the Taklimakan Desert, checkerboard barriers, fences, and netting have been constructed to protect a major highway from dune encroachment (Dong *et al.*, 2004; Lei *et al.*, 2008). Studies in Shapotou and Taklimakan showed that shelterbelts are the best solution (Mitchell *et al.*, 1998; Sørensen, 2004). However, the QTR is built in an alpine region, which can not support shelterbelts. As the climate warms, and as the intensity of anthropogenic activities and associated pest populations continue to increase, shallow permafrost freezing and thawing processes will intensify, creating

freeze-thaw desertification (Livingstone *et al.*, 2007; Wu *et al.*, 2008). Therefore, sand damage along the QTR is expected to become increasingly serious.

Since the beginning of construction of the QTR, the sand-control measures have played an important role for the safe operation of the railway. The SCB and the SF are two of the most effectively sand-control measures of the QTR. This paper simulated the embankments, SCBs and SFs of the QTR in a wind tunnel, and analyzed their respective wind profile, sand deposition, and the SBR in conjunction with field data. Construction of the railway and sand prevention system greatly changed the blown sand transport of the primary surface. Wind speed increased by 67.7%–77.3% at the upwind shoulder of the embankment and decreased by 50.0%–83.3% at upwind foot of embankment. The SF reduced wind speed by 50.0%–100.0% after passing through the first fence. In the experiments with the SCBs, the wind speed decreased by 72.2%–100.0% after the first row of stones within the first SCB grid. The higher the wind speed, the lower the SBR of the SCB and SF. From field investigation, the amount of sand blocked by the four SFs decreases exponentially. Although the SCB can only block lower amounts of sand, it has a higher SBR (96.7%) than that of SF (50.0%).

The SFs and SCBs along the Golmud-Lhasa section of the QTR provide an obvious sand blocking effect. However, sand that is originally scattered and distributed sparsely across large areas of sandy grassland is blocked by sand-prevention measures and transferred towards the railway. When it becomes concentrated and accumulates, a 100–200-m-wide artificial dune is formed on both sides of the railway, and it is becoming a new source of sand damage. The control of sand damage through prevention rather than treatment is the preferred option, and stabilizing the sand source dunes is a better long-term method of prevention.

## Acknowledgement

The authors thank Susan Cook and Cactus Communications Company for editing the manuscript in English.

## References

Alghamdi A A A, Al-Kahtani N S, 2005. Sand control measures and sand drift fences. *Journal of Performance of Constructed Facilities*, 19(4): 295–299. doi: 10.1061/(ASCE)0887-3828(2005)19:4(295)

Bai Huzhi, Li Dongliang, Dong Anxiang, 2005. Strong wind and wind pressure along the Qinghai-Tibet Railway. *Journal of Glaciology and Geocryology*, 27(1): 111–116. (in Chinese)

Bai Yang, Wang Nai′ang, Liao Kongtai *et al*., 2011. Geomorphological evolution revealed by aeolian sedimentary structure in Badain Jaran Desert on Alxa Plateau, Northwest China. *Chinese Geographical Science*, 21(3): 178–187. doi: 10.1007/s11769-011-0468-y

Chang Zhaofeng, Zhong Shengnian, Han Fugui *et al*., 2000. Research of the suitable row spacing on clay barriers and straw barriers. *Journal of Desert Research*, 20(4): 455–457. (in Chinese)

Chen Hui, Li Shuangcheng, Zhang Yili, 2003. Impact of road construction on vegetation alongside Qinghai-Xizang highway and railway. *Chinese Geographical Science*, 13(4): 340–346. doi: 10.1007/ s11769-003-0040-5

Cheng G D, Sun Z Z, Niu F J, 2008. Application of the roadbed cooling approach in Qinghai-Tibet railway engineering. *Cold Regions Science and Technology*, 53(3): 241–258. doi: 10.1016/j.coldregions.2007.02.00

Cheng G D, Wu T H, 2007. Responses of permafrost to climate change and their environmental significance, Qinghai-Tibet Plateau. *Journal of Geophysical Research*, 112(F2): 1–10. doi: 10.1029/2006JF000631

Dong Z B, Chen G T, He X D *et al*., 2004. Controlling blown sand along the highway crossing the Taklimakan Desert. *Journal of Arid Environments*, 57(3): 329–344. doi: 10.1016/j.jaridenv.2002.02.001

Han Q J, Qu J J, Dong Z B *et al.*, 2013. The effect of air density on sand transport structures and the adobe abrasion profile: A field wind-tunnel experiment over a wide range of altitude. *Boundary-layer Meteorology*, 150(2): 299–317. doi: 10.1007/s10546-013-9874-2

Han Zhiwen, Wang Tao, Dong Zhibao *et al*., 2004. Main engineering measurements and mechanism of blown sand hazard control. *Progress in Geography*, 23(1): 13–21. (in Chinese)

Jin H J, Wei Z, Wang S L *et al*., 2008. Assessment of frozen-ground conditions for engineering geology along the Qinghai-Tibet highway and railway, China. *Engineering Geology*, 101(3–4): 96–109. doi: 10.1016/j.enggeo.2008.04.001

Lei J Q, Li S Y, Fan D D *et al*., 2008. Classification and regionalization of the forming environment of windblown sand disasters along the Tarim Desert Highway. *Chinese Science Bulletin*, 53(2): 1–7. doi: 10.1007/s11434-008-6023-2

Liu Z M, Zhao W Z, 2001. Shifting sand control in central Tibet. *Ambio*, 30(6): 376–380

Livingstone I, Wiggs G F S, Weaver C M, 2007. Geomorphology of desert sand dunes: A review of recent progress. *Earth Science Reviews*, 80(3–4): 239–257. doi: 10.1016/j.earscirev.2006.09.004

Ma W, Cheng G D, Wu Q B, 2009. Construction on permafrost foundations: Lessons learned from the Qinghai-Tibet railroad. *Cold Regions Science and Technology*, 59(1): 3–11. doi: 10.1016/j.coldregions.2009.07.007

Mitchell D J, Fullen M A, Trueman I C *et al*., 1998. Sustainability of reclaimed desertified land in Ningxia, China. *Journal of Arid Land*, 39(2): 239–251. doi: 10.1006/jare.1998.0396

Qiu G Y, Lee I B, Shimizu H *et al*., 2004. Principles of sand dune fixation with straw checkerboard technology and its effects on the environment. *Journal of Arid Environments*, 56(3): 449–464. doi: 10.1016/S0140-1963(03)00066-1

Qu Jianjun, Lin Yuquan, Liu Xianwan *et al*., 2002. The effects of an A-typed nylon fence on Aeolian sand prevention. *Journal of Lanzhou University* (*Natural Sciences*), 38(2): 171–176. (in Chinese)

Sørensen M, 2004. On the rate of aeolian sand transport. *Geomorphology*, 59(1–4): 53–62. doi: 10.1016/j.geomorph.2003.09.005

Wu Q B, Lu Z J, Zhang T J *et al.*, 2008. Analysis of cooling effect of crushed rock-based embankment of the Qinghai-Xizang Railway. *Cold Regions Science and Technology*, 53(3): 271–282. doi: 10.1016/j.coldregions.2007.10.004

Wu Q B, Shi B, Fang H Y, 2003. Engineering geological characteristics and processes of permafrost along the Qinghai-Xizang Highway. *Engineering Geology*, 68(3–4): 387–396. doi: 10.1016/S0013-7952(02)00242-9

Wu Q B, Zhang T J, 2010. Changes in active layer thickness over the Qinghai-Tibetan Plateau from 1995 to 2007. *Journal of Geophysical Research*, 115(D9): D09107. doi: 10.1029/2009JD012974

Xie S B, Qu J J, Zu R P *et al.*, 2012. New discoveries on the effects of desertification on the ground temperature of permafrost and its significance to the Qinghai-Tibet Plateau. *Chinese Science Bulletin*, 57(8): 838–842. doi: 10.1007/s11434-011-4901-5

Xu X L, Zhang K L, Kong Y P *et al*., 2006. Effectiveness of erosion control measures along the Qinghai-Tibet highway, Tibetan Plateau, China. *Transportation Research Part D*: *Transport and Environment*, 11(4): 302–309. doi: 10.1016/j.trd.2006.06.001

Yang M X, Wang S L, Yao T D, 2004. Desertification and its relationship with permafrost along the Qinghai-Tibet Plateau. *Cold Regions Science and Technology*, 39(1): 47–53. doi: 10.1016/j.coldregions.2004.01.002

Ying Daiying, Qu Jianjun, Han Qingjie *et al*., 2013. Wind-blown sand activity intensity in Cuonahu Lake section of Qinghai-Tibet Railway. *Journal of Desert Research*, 33(1): 9–15. (in Chinese)

Zhang C L, Zou X Y, Pan X H *et al*., 2007. Near-surface airflow field and aerodynamic characteristics of the railway-protection system in the Shapotou region and their significance. *Journal of Arid Environments*, 71(2): 169–187. doi: 10.1016/j.jaridenv.2007.03.006

Zhang K C, Qu J J, Han Q J *et al*., 2012. Wind energy environments and aeolian sand characteristics along the Qinghai-Tibet Railway, China. *Sedimentary Geology*, 273–274: 91–96. doi: 10.1016/j.sedgeo.2012.07.003

Zhang K C, Qu J J, Liao K T *et al*., 2010. Damage by wind-blown sand and its control along Qinghai-Tibet Railway in China. *Aeolian Research*, 1(3–4): 143–146. doi: 10.1016/j.aeolia.2009.10.001

Zhang Kecun, Qu Jianjun, Niu Qinghe *et al*., 2011. Protective mechanism and efficiency of sand-blocking fence along Qinghai-Tibet Railway. *Journal of Desert Research*, 31(1): 16–20. (in Chinese)

Zou X Y, Li S, Zhang C, 2002. Desertification and control plan in the Tibet Autonomous Region of China. *Journal of Arid Environments*, 51(2): 183–198. doi: 10.1006/jare.2001.0943